Proceedings of ASME Turbo Expo 2011
GT2011
June 6-10, 2011, Vancouver, British Columbia, Canada

GT2011-45362

EXPERIMENTAL INVESTIGATION OF TURBULENT BOUNDARY LAYER FLASHBACK LIMITS FOR PREMIXED HYDROGEN-AIR FLAMES CONFINED IN DUCTS

Christian Eichler*, **Georg Baumgartner, Thomas Sattelmayer**

Lehrstuhl für Thermodynamik
Technische Universität München
D-85747 Garching, Germany
Email: eichler@td.mw.tum.de

ABSTRACT

The design of flashback-resistant premixed burners for hydrogen-rich fuels is strongly dependent on reliable turbulent boundary layer flashback limits, since this process can be the dominant failure type for mixtures with high burning velocities. So far, the flashback data published in literature is based on tube burner experiments with unconfined flames. However, this flame configuration may not be representative for the most critical design case, which is a flame being already present inside the duct geometry. In order to shed light on this potential misconception, boundary layer flashback limits have been measured for unconfined and confined flames in fully premixed hydrogen-air mixtures at atmospheric conditions. Two duct geometries were considered, a tube burner and a quasi-2D turbulent channel flow. Furthermore, two confined flame holding configurations were realized, a small backward-facing step inside the duct and a ceramic tile at high temperature, which was mounted flush with the duct wall. While the measured flashback limits for unconfined tube burner flames compare well with literature results, a confinement of the stable flame leads to a shift of the flashback limits towards higher critical velocity gradients, which are in good agreement between the tube burner and the quasi-2D channel setup. The underestimation of flashback propensity resulting from unconfined tube burner experiments emerges from the physical situation at the burner rim. Heat loss from the flame to the wall results in a quenching gap, which causes a radial leakage flow of fresh gases. This flow in turn tends to increase the quenching distance, since it constitutes an additional convective heat loss. On the one hand, the quenching gap reduces the local adverse pressure gradient on the boundary layer. On the other hand, the flame base is pushed outward, which deters the flame from entering the boundary layer region inside the duct. The flashback limits of confined flames stabilized at backward-facing steps followed this interpretation, and experiments with a flush ceramic flame holder constituted the upper limit of flashback propensity. It is concluded that the distribution of the flame backpressure and the flame position itself are key parameters for the determination of meaningful turbulent boundary layer flashback limits. For a conservative design path, the present results obtained from confined flames should be considered instead of unconfined tube burner values.

INTRODUCTION

The capability of burning highly reactive fuels in a fully premixed, undiluted mode has become a main development focus in the gas turbine industry. While such systems are the natural response to current energy market demands, which comprise fuel flexibility towards hydrogen-containing fuels, low NOx emissions and optimized plant efficiencies, the realization of stable and safe combustion is a challenging task under such circumstances. The prevention of flame flashback inside the wall-near

*Address all correspondence to this author.

regions of fuel-supply ducts is especially challenging because there are only limited data and methods available to predict this failure type for a given geometry. During a typical design process, the critical velocity gradient model from the work of Lewis and von Elbe [1] is used as a starting point. Their results from laminar tube burner experiments showed that the stability limit is independent of tube Reynolds number Re_d (except for very small diameter tubes) if expressed by the velocity gradient $\partial u/\partial y$ right at the wall upstream of the stable flame position. The critical gradient model includes the flame speed and a measure of the quenching distance from the wall during flashback as variables. Since the second quantity is generally difficult to calculate a priori, especially for turbulent flows, developers refer to experimental data to obtain critical gradients for specific fuel mixtures or for pure fuels and subsequent conversion to the desired mixture fractions (see [2] for an interpolation scheme example). Furthermore, the results have to be scaled to realistic preheat temperatures and pressures [3–5]. The critical gradients are finally used to derive minimum mean flow velocities in the fuel supply ducts in order to avoid boundary layer flashback during normal operation. It is clear that these supply velocities have an upper limit determined by the main flame stabilization method, and that the security factor may not be very high for hydrogen-containing fuels.

The design procedure outlined above is straightforward. However, it is not clear whether this procedure also provides for safety margins regarding a flame which has accidentally entered the fuel supply, e.g. due to an intermittent velocity drop or due to self-ignition, and which is burning there inside the boundary layer region and has to be washed out again. The uncertainty arises from a different geometrical configuration in the region of interaction between flame and incoming boundary layer flow inside the duct, which will be referred to as a confined situation in the following, when compared to the stable flame position, which is mostly preceded by a step change in cross-section. The fundamental question is whether the flashback limits are the same for these two different cases or not. It has been recently documented [6] that published laminar and turbulent boundary layer flashback limits in generic configurations are exclusively derived from tube or slit burners with an open atmosphere or large area ratio boundary condition at the burner exit. Thus, there is no experimental or numerical evidence available so far to assess the validity of critical gradients from unconfined experiments with respect to a flashback-safe burner design.

An experimental approach has been chosen in the present work to investigate the potential misconception described above. In a first step, turbulent flashback limits are measured for atmospheric hydrogen-air mixtures in an unconfined tube burner for comparison with literature results. Secondly, flashback limits are measured in a quasi-2D channel flow, which represents the confined situation of a flame already burning inside a duct. Finally, the tube burner is modified to allow the flame to enter the tube prior to flashback, which is comparable to the physical situation inside the channel setup.

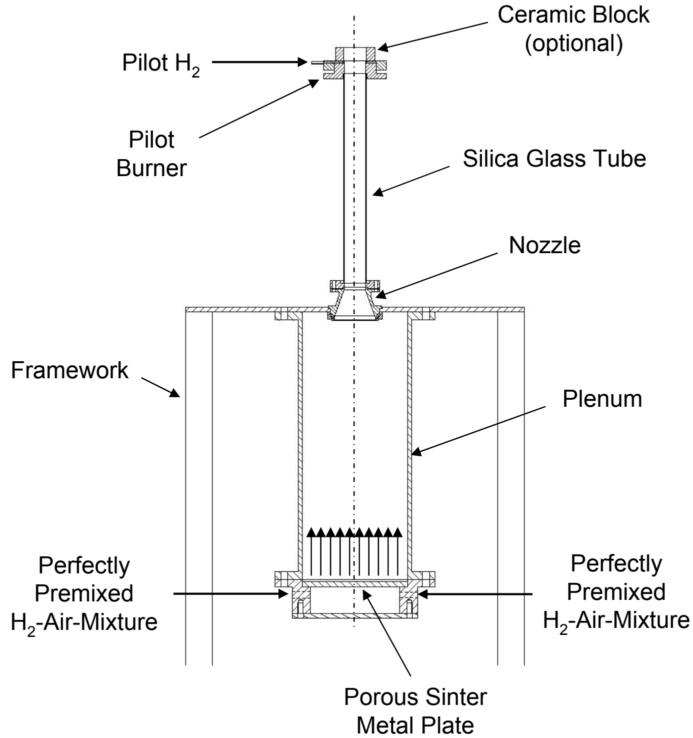

Figure 1: TUBE BURNER RIG.

EXPERIMENTAL SETUP

The tube burner and channel setups will be described in this section along with experimental and numerical representations of the flow field inside the rigs.

Tube Burner Setup

A schematic of the tube burner rig is shown in Fig. 1. Hydrogen and air are perfectly premixed far upstream of the burner section using a static flow mixer. The mixture enters a large-volume plenum through a sinter metal plate at the bottom, which acts as flow straightener and flashback arrestor at the same time. The fluid is subsequently accelerated into a silica glass tube by means of a nozzle and the velocity profile develops toward the tube exit, where the reactive mixture is ignited by a concentric pilot burner. The diameter of the tube is constant at 40 mm and its length amounts to 400 mm. Both the air mass flow rate and the hydrogen mass flow rate are controlled by Bronkhorst thermal mass flow controllers with maximum mass flow deviations of $\pm$ 1 %. The tube diameter of 40 mm has been chosen for two reasons: (1) the small curvature of the rather large tube

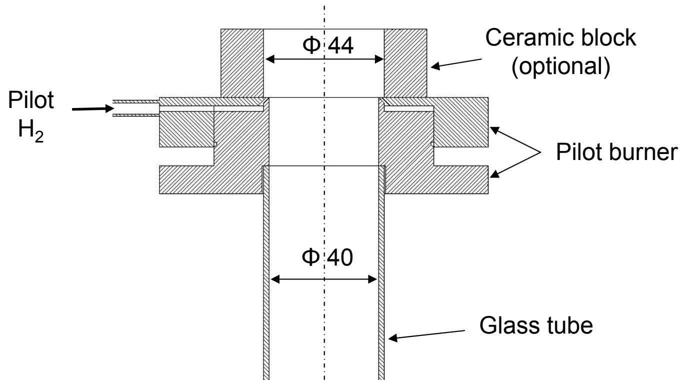

Figure 2: DETAILS OF TUBE EXIT AND PILOT BURNER (DIMENSIONS IN MM).

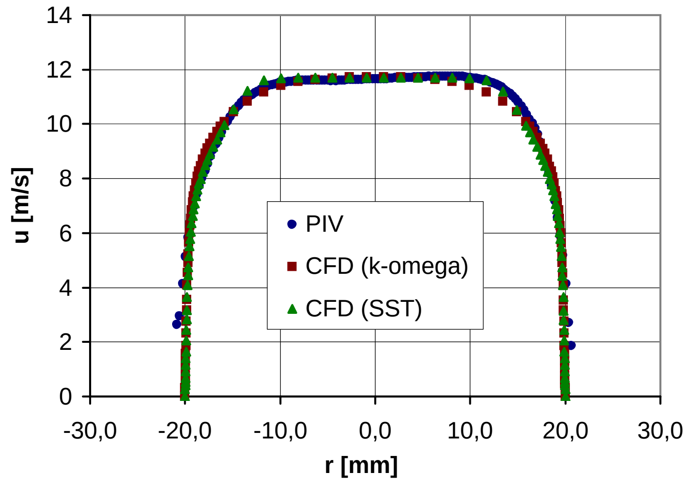

Figure 3: VELOCITY PROFILES AT TUBE BURNER OUTLET.

yields minimal mutual interaction of the boundary layer sections around the circumference of the tube; (2) the flashback limits determined for the 40 mm tube are well comparable to those of a 38 mm tube documented in [7]. The design of the tube exit and pilot burner is shown in Fig. 2. Pure hydrogen is injected into the main gas flow under an angle of 45° through an annular slot of 1mm width. This helps to stabilize the flame under normal operating conditions. The pilot gas flow is switched off when approaching flashback to avoid any influence on the flashback limits.

Part of the tube burner experiments were conducted with a concentric ceramic block downstream of the pilot burner, which had a streamwise extension of 30 mm and an inner diameter of 44 mm. While in the open tube configuration the flame is stabilized in the shear layers above the pilot burner rim, the flame no longer stays in that region with the ceramic block on top of the burner. The rough surface of the ceramic allows parts of the flame to creep upstream during stable operation and finally to stabilize at the original burner rim, representing the case that a flame is already present well inside the duct. The configuration with ceramic block will be referred to as the *confined* case, since the flame is burning inside the ceramic duct well before flashback. The tube burner without ceramic block will be referred to as the *unconfined* case.

K-type thermocouples were used to measure the temperature of the burner tip and the glass tube. During long-term operation without any cooling the temperature of the pilot burner rose up to approximately 120 °C for the unconfined setup and up to approximately 230 °C for the confined setup, respectively. This caused rather poor reproducibility of the test results because for a certain mass flow rate the equivalence ratio at flashback decreased by as much as $\delta\phi = -0.05$ for increasing burner tip temperatures. This temperature dependence applied in particular to the confined case, whereas it was almost negligible for the moderate temperature rise in the unconfined case. This observation is in accordance with a remark in [1], where the authors stated that atmospheric flashback results are little affected by an increase in tube temperature up to 100 °C. Own experience from the experiments in [6] confirms this statement. To obtain reproducible results for both setups, the pilot burner was convectively cooled by three air jets impinging on its circumferential surface in 120° angles. In this way, the temperature of the pilot burner, which is made from brass, could be kept between 40 and 60 °C during all operating conditions.

Tube Burner Flow Field

Due to the small length-to-diameter ratio of the glass tube, the shape of the velocity profile at the tube outlet is not known a priori. In order to obtain realistic velocity gradients, a combined experimental and numerical approach was chosen. First, the velocity profile above the burner exit was measured by means of Particle Image Velocimetry (PIV). The measured profile was then compared to a Reynolds-Averaged Navier-Stokes (RANS) simulation, and the quality of the match in the wake region of the boundary layer and the core flow field was assumed to be an indicator for the agreement of the wall friction between measurement and simulation. For the PIV experiments, TiO_2 seeding particles were injected into the flow inside the plenum (cf. Fig. 1). The data evaluation was performed with interrogation areas of size 32x32 pixels and an overlap of 75 %. The RANS simulations were performed in ANSYS CFX using two different two-equation turbulence models - the k-ω model and the SST model. In both cases, the wall boundary layer was fully resolved. The resulting experimental and CFD velocity profiles at the tube burner exit for a bulk flow velocity of 10 m/s are exemplarily shown in Fig. 3. Aside from minor discrepancies, the experi-

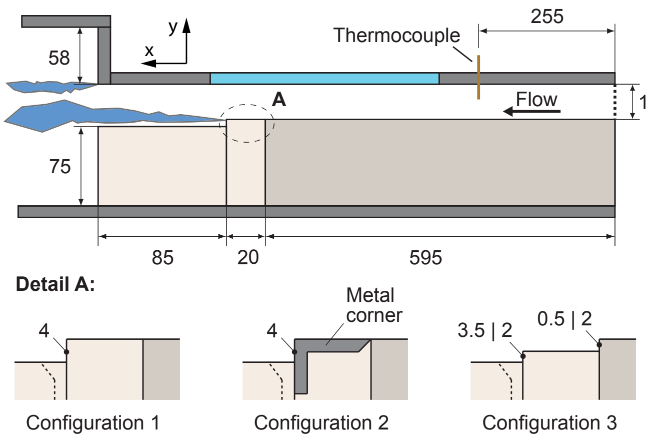

Figure 4: CHANNEL MEASUREMENT SECTION (DIMENSIONS IN MM).

mental results and the simulations match very well in the outer boundary layer region and the core flow. Deviations are observed in the region where the shear layer between particle-laden flow and atmosphere has started to deform the boundary layer profile in the experiment. The simulation using the SST turbulence model, which is known to combine the good near-wall behavior of the k-ω model and the excellent far-field behavior of the k-ε model, shows a slightly better match to the experiment and has been chosen for all following comparisons. It is concluded from Fig. 3 and analogous results from measurements at various bulk flow velocities that the velocity gradients at the wall are accurately represented by the RANS simulations.

In a next step, the RANS velocity gradients were compared to predictions from the Blasius correlation for fully developed turbulent pipe flow [8]:

$$g = \frac{\tau_w}{\mu} = 0.03955\,\bar{u}^{\frac{7}{4}}\,\nu^{-\frac{3}{4}}\,d^{-\frac{1}{4}} \tag{1}$$

In Eq. 1, g is the velocity gradient at the wall, τ_w is the wall shear stress, μ and ν are the dynamic and kinematic viscosity of the mixture, respectively, d is the pipe diameter and $\bar{u}$ is the bulk flow velocity. Although the flow in the experimental setup is not fully developed, it could be shown that this has no appreciable effect on the velocity gradients at the wall (mean errors lay within ±4 %), i.e. that the latter can be calculated from the correlation of Eq. 1.

Channel Setup

The experimental infrastructure of the channel setup with regard to fuel-air premixing, flow straightening, inflow velocity profile, boundary layer manipulation in the edges of the channel by air blowing and pilot burners has been described elsewhere [6]. Figure 4 illustrates the key features of the present channel measurement section. In the upper part of the figure, a midplane cross-section through the flow path is shown. The perfectly premixed hydrogen-air mixture enters the duct from the right through a fine-wire mesh, which is the last one of a series of flow straightening devices (please note that the inlet velocity profiles shown in [6] were measured 150 mm downstream of this last mesh). The duct has a height of 17.5 mm and a constant lateral width of 157 mm, which results in an aspect ratio high enough to ensure quasi-2D flow characteristics in a large lateral portion of the channel. The upper wall of the duct is formed by a stainless steel plate with a window port towards the end of the section. The window insert is mounted flush with the upper wall. The lower wall is formed by a machined stainless steel block. The lower wall is cooled by three air jets impinging on the wall from below inside of the block at its downstream end, which is located next to the flame anchoring position. The cooling air convects in the upstream direction inside the block and leaves the cavity through a bore hole at the upstream end of the block. The surface temperature of the lower wall is monitored by type K thermocouples at three axial locations at the lateral center position. The thermocouples are inserted into blind holes inside of the block. During experiments, the maximum measured wall temperatures lay below 40 °C, which satisfies the criterion for negligible influence on the flashback process at atmospheric conditions as discussed before. The duct sidewalls are partly formed by stainless steel plates as well as window ports on each side. The side windows are approximately located at the same axial position as the upper window. After a length of 595 mm, a ceramic tile of 20 mm streamwise extension is attached to the metal block. Downstream of the tile, a small pilot flame emerges through a slot of approximately 2 mm axial width, which ignites the reactive mixture inside the duct. Another ceramic block of 85 mm in length is attached to the tile. The detailed configuration of tile and block is shown in the lower part of Fig. 4. In configuration 1, the tile is flush with the steel block, and the ceramic block has an offset of 4 mm. The dotted lines represent the slit of the pilot burner. Configuration 2 has the same dimensions, but a stainless steel corner has been mounted onto the tile. The corner is sharpened on its upstream end in order to minimize the thermal contact between corner and steel block. In configuration 3, the ceramic tile is offset by either 0.5 or 2 mm, which results in an offset between ceramic block and tile of 3.5 or 2 mm, respectively. At the end of the ceramic block, a sudden area increase leads into the combustion chamber, where a second pilot burner is located at the upper edge. The aerodynamic design of the measurement section makes sure that during flashback, the flame only propagates along the lower wall. The fuel is shut down once that the flame reaches the thermocouple located 255 mm downstream of the last wire mesh.

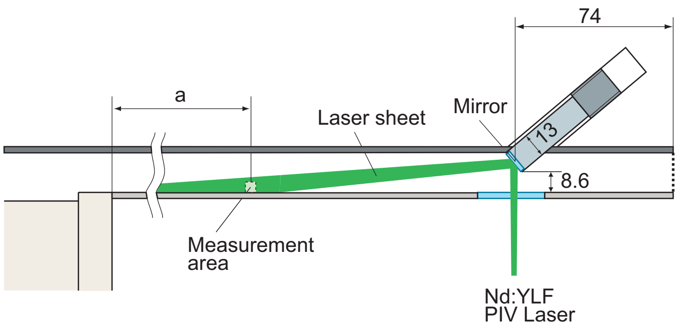

Figure 5: PIV CONFIGURATION FOR BOUNDARY LAYER MEASUREMENTS (DIMENSIONS IN MM).

Channel Flow Field

Since the duct length for premixed combustion experiments is limited due to the risk of deflagration-detonation transition, the channel length of 595 mm is not sufficiently long to establish a fully developed turbulent velocity profile over the majority of its axial length. Thus, for similar reasons as in the tube burner setup, isothermal flow velocities were measured to get an estimate of the actual velocity gradients at the lower wall. The PIV technique was chosen for the velocity measurements, since it opens up the possibility of measurements during flashback, with the density gradient of the seeding as a marker of the flame position. However, only isothermal results are presented here for the time being.

In order to resolve the boundary layer right down to the wall, a special setup was designed which inserts the light sheet parallel to the wall. The components are sketched in Fig. 5. At a distance of 74 mm downstream of the last grid, a small window port is located at the bottom wall. This window is again mounted flush with the wall. On the top wall, a cylinder of 13 mm diameter extends into the flow. Although this configuration clearly leads to a certain flow displacement, it is considered as acceptable here for two reasons: (1) The disturbance is located on the upper wall, which is not the place where flashback is occurring, and (2) the overall blockage is very small, namely 3.7 % when comparing the projected cylinder area and the duct cross-section. The cylinder has a fine thread on its upper end for linear adjustment. On its lower end, a mirror is mounted, which deflects the laser sheet towards the axial direction of the channel. Due to this alignment, the reflections on the machined lower channel wall only have a negligible extension into the flow field, and meaningful measurements can be taken down to the laminar sublayer for the flow velocities considered here. The measurement area has a size of approximately 5x5 mm and was recorded by a 1024x1024 pixel CMOS Photron SA5 camera. An Infinity K2/S Long Distance Microscope was used as lens, which has been shown to be a proper optical instrument for μ-PIV investigations in turbulent boundary layers [9]. The axial location of the center of the measurement area is given by the distance a. Three axial positions with $a = 246$, 134 and 32 mm have been chosen for the flow characterization. The flow was globally seeded by injection of TiO_2 aerosol upstream of the fuel injection point. The PIV data was analyzed with an adaptive cross correlation method, and 8x8 pixels interrogation areas with 50 % overlap have been used. Due to the small size of the interrogation areas in terms of wall units (cf. Eq. 2), bias errors due to deviations of the local section of the velocity profile from a constant gradient slope inside the interrogation areas can be neglected.

The results of the PIV boundary layer measurements are shown in Figs. 6. Two air massflow rates have been considered, 30 g/s (Fig. 6a) and 60 g/s (Fig. 6b). Velocity profiles of the mean axial velocity u are shown at three axial locations a as described earlier. It can be seen that the wall-near region up to about $y = 1$ mm is in very good agreement throughout the measurements. For the 30 g/s case, Fig. 6a reveals that the boundary layer profile is still subject to minor changes between $a = 246$ mm and $a = 134$ mm, which can be ascribed to the lower duct Reynolds number and the resulting lower turbulence level in the developing boundary layer. Since the wall velocity gradient is believed to be the determining factor for turbulent flashback limits (this assumption still has to be proved, see comments in [6]), these gradients have been determined from the first derivative of a linear fit through the PIV measurement points within the laminar sublayer, which can be characterized by [10]:

$$y^+ \leq 5\,, \qquad \text{where} \quad y^+ = \frac{y}{\nu} u_\tau \tag{2}$$

In Eq. 2, ν is the kinematic viscosity of the mixture and u_τ is the shear stress velocity, calculated from the wall shear stress τ_w and the mixture density ρ by $u_\tau = \sqrt{\tau_w/\rho}$. Since τ_w is calculated by the gradients g from the PIV velocity data, the linear fit inside the sublayer is an iterative procedure. The resulting velocity gradients have been compared to the wall friction of fully-developed channel flow between two parallel plates. A log-law approximation of the velocity profile across the entire channel can be integrated to give a relation between the average channel velocity u_{av} and the friction velocity [10]:

$$u_{av} = u_\tau \left(\frac{1}{\kappa} \ln \frac{h\, u_\tau}{\nu} + \mathrm{B} - \frac{1}{\kappa} \right) \tag{3}$$

In Eq. 3, the variable h is the half channel height, and $\kappa = 0.41$ and $\mathrm{B} = 5$ have been assumed here. From this relation, the velocity gradient g, which is contained in u_τ, can be iteratively calculated.

The comparison of wall velocity gradients derived from the PIV data and the results of Eq. 3 is displayed in Fig. 7. At the

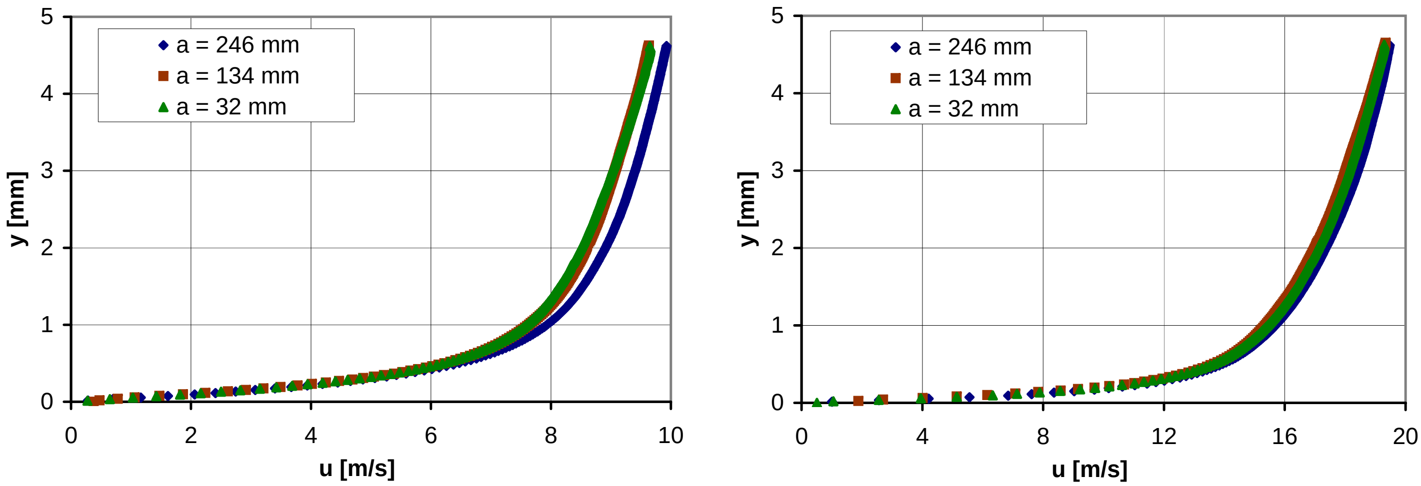

(a) PROFILES FOR 30 G/S AIR MASSFLOW.

(b) PROFILES FOR 60 G/S AIR MASSFLOW.

Figure 6: MEAN BOUNDARY LAYER VELOCITY PROFILES AT THREE AXIAL LOCATIONS.

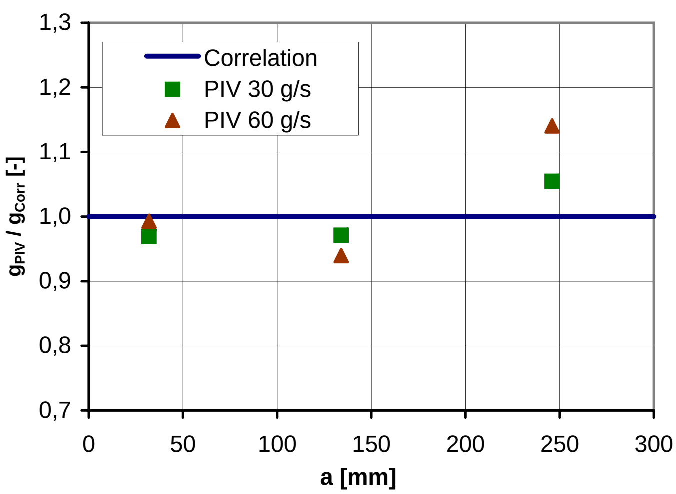

Figure 7: COMPARISON OF VELOCITY GRADIENTS FROM PIV RESULTS AND CORRELATION.

location $a = 246\,\mathrm{mm}$, the measured gradients lay above the correlation value. Further downstream, the gradients adjust towards the correlation value and only differ by -6 % or less from the correlation. It is concluded that the gradients g determined from Eq. 3 provide a satisfactory representation of the experiment within an approximate error band of ± 10 %.

MEASUREMENT PROCEDURE

Boundary layer flashback limits were recorded for both the tube burner and the channel setup in a similar fashion. At the beginning of each single measurement the rigs were operated in stable mode, using the pilot burners to stabilize the flame. During the approach towards flashback, the air mass flow rate was kept constant while the hydrogen mass flow rate was increased, starting from lean conditions, in little steps until flashback occurred. After each stepwise increase in hydrogen mass flow rate, the setups were operated for a sufficiently long time to be sure mass flow oscillations had leveled off. The pilot burners were shut off as soon as a self-stabilization of the main flame was possible, which always occurred well before the flashback point. The whole process was monitored by an intensified charge-coupled device (ICCD) camera (Hamamatsu C4336-02), which received mainly the OH*-chemiluminescence through the use of an interference UV filter and a silica lens in both cases. The flashback limit was defined as the equivalence ratio Φ when the flame started to propagate upstream along the wall boundary layer, i.e. when an OH*-chemiluminescence signal could be detected inside the glass tube or parts of the flame went beyond the steel block edge in the channel case. The corresponding critical velocity gradients g_c were subsequently calculated from Eqs. 1 or 3, respectively.

The flame holding in the tube burner setups is shown in Fig. 8a. Here, three images are superimposed - the instantaneous OH* intensities of the unconfined and the confined flame above the pilot burner and above the ceramic block, respectively, along with an image of the pilot burner at ambient light. The OH* images were recorded at an exposure time of 1 ms and the edges of the ceramic block are marked by white lines. Two observations can be made: (1) the line-of-sight integrated OH* signal near the flame base is most intense in the far left and the far right of the image, indicating that the flame is stabilized in the shear layers above the pilot burner; (2) the flame in the confined case is not

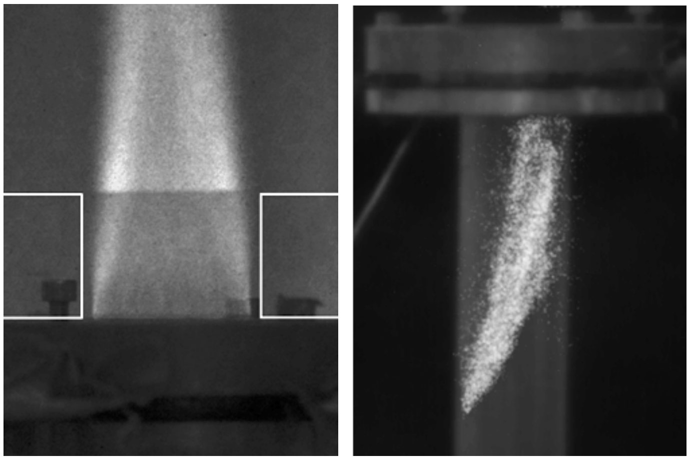

(a) UNCONFINED AND CONFINED STABLE FLAMES. (b) FLAME AT FLASHBACK.

Figure 8: FLAME STABILIZATION BEFORE (A) AND DURING (B) FLASHBACK (TUBE BURNER).

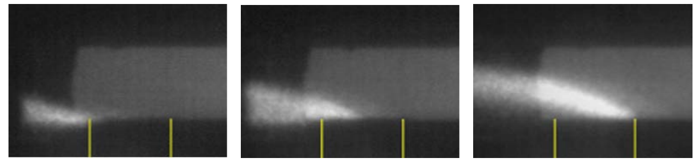

(a) WAKE STABILIZATION. (b) UPSTREAM CREEP ON CERAMIC TILE. (c) STABILIZATION ON CERAMIC TILE.

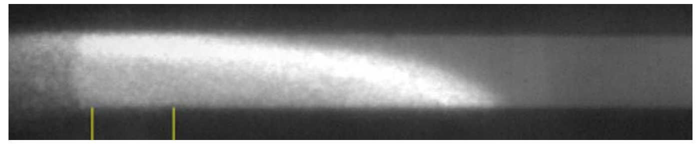

(d) FLAME AT FLASHBACK.

Figure 9: FLAME STABILIZATION BEFORE (A-C) AND DURING (D) FLASHBACK (CHANNEL, CONFIGURATION 1).

stabilized above the ceramic block because there is a rather large gap between the upper edge of the ceramic block and the OH* signal detected at this position. By contrast, the diameter of the flame cone in the confined case coincides well with the one in the unconfined case, implying that the flame is stabilized above the pilot burner in both setups. Fig. 8b shows an instantaneous image of the flame flashing back along the wall boundary layer on the left side of the tube.

The evolution of the flame stabilization from piloted operation to flashback for configuration 1 of the channel case is illustrated by instantaneous flame images in Figs. 9. The images show overlays of the flame OH* signal captured with the ICCD camera at an exposure time of 1 ms with an image of the measurement section at ambient light. The axial extent of the ceramic tile is marked by vertical yellow lines in each figure. In Fig. 9a, the flame is stabilized in the wake of the ceramic tile. The pilot burner was shut off at this point. On further increase of the fuel mass flow rate, the flame creeps upstream along the rough surface of the ceramic tile as shown in Fig. 9b. Some seconds before flashback, the flame stabilizes at the upstream end of the ceramic tile (Fig. 9c). Figure 9d shows the flame during flashback through the channel. Based on the explanations for Figs. 8 and 9, the observed stabilization mechanisms prior to flashback (cf. Fig. 9c) were three-fold for the different duct geometries considered: (1) Wake stabilization downstream of the burner rim without ceramic block or downstream of the metal corner in configuration 2 of the channel case, (2) thermal stabilization on the rough ceramic surface for configuration 1 of the channel case, or (3) a combination of both for the tube burner with ceramic block and configuration 3 of the channel case.

RESULTS AND DISCUSSION

The results of the flashback measurements are summarized in Fig. 10. In Fig. 10a, the flashback limits of the unconfined tube burner are compared to literature values from [7]. In Fig. 10b, the flashback limits of the three different configurations of the channel setup are compared to confined tube burner limits. Furthermore, the unconfined tube burner limits from Fig. 10a are included again.

It can be clearly seen in Fig. 10a that the literature values for $d = 38\,\mathrm{mm}$ could be reproduced accurately over a wide range of equivalence ratios with the current setup. These results underline the suitability of the experimental rig and the used velocity gradient correlation for meaningful flashback measurements in the unconfined case.

Turning to the flashback limits of the channel setup, which are shown in Fig. 10b, monotonously increasing critical gradients for increasing fuel mixture fraction are also observed for all configurations in this case. However, the critical gradients lie substantially above the unconfined tube burner values, approaching almost one order of magnitude in difference towards stoichiometry. A trend regarding the influence of the backward-facing step used as flame holder can be determined by comparing the limits between configurations 1 and 3. The flashback limits of configuration 3 with a 0.5 mm step lie consistently below the flush case represented by configuration 1 for lean mixtures. Close to $\Phi = 1$, the difference vanishes. For configuration 3 with a 2 mm step, only three different air massflows have been considered, which nevertheless confirm the trend towards lower flashback susceptibility with increasing step height. An offset of the first three sets of points towards leaner conditions can be observed for configurations 1 and 3. This can be explained by the flashback behavior of the rig in this region. The flame passed the line between ceramic tile and steel block only slightly at the

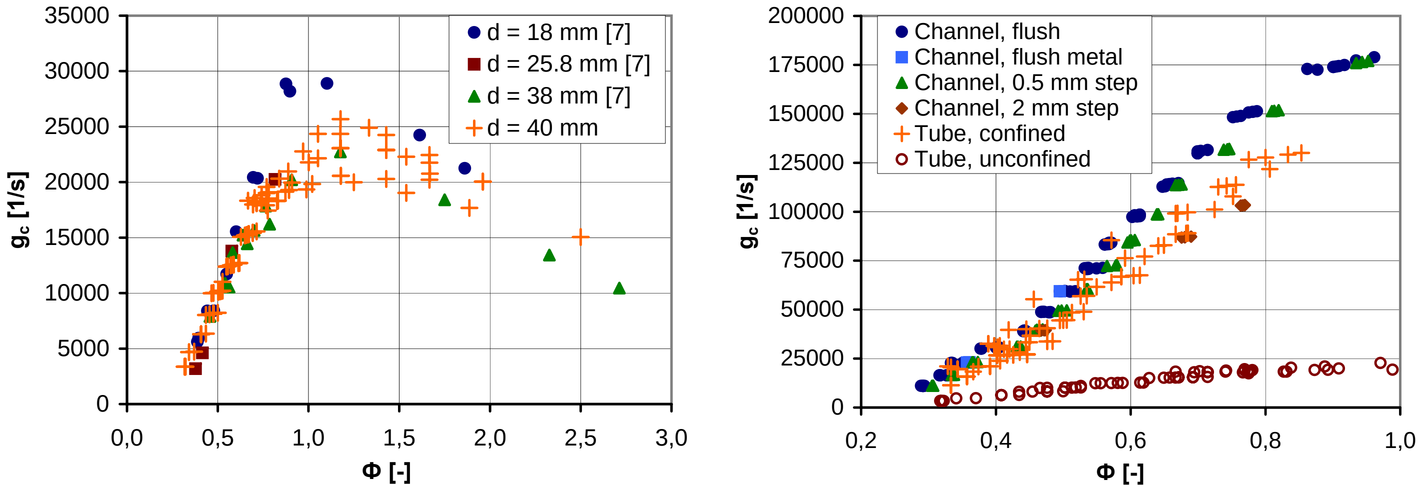

(a) TUBE BURNER WITHOUT CONFINEMENT. (b) TUBE BURNER WITH CONFINEMENT AND CHANNEL.

Figure 10: BOUNDARY LAYER FLASHBACK LIMITS FOR CONFINED AND UNCONFINED HYDROGEN-AIR FLAMES.

beginning, moving back and forth. According to the definition given in the experimental procedure, this point was regarded as the flashback limit. By increasing the fuel massflow, the flame moved further upstream, until it finally reached the position of the thermocouple. For higher Φ, flashback was a sudden event, and thus more clearly defined. The influence of the surface material of the 20 mm portion downstream of the steel block, either ceramic in configuration 1 or metal in configuration 2, is obviously negligible, since both cases show the same flashback limit for a given flow velocity. It should be mentioned that only two flashback points could be accurately determined using the metal corner because of thermoacoustic instabilities, which arose at all other tested air massflows. The flame started flickering back and forth on the metal corner surface well before the flashback point, which triggered the instability. In contrast, the low heat conductivity of the ceramic block resulted in a high surface temperature above the self-ignition temperature of the mixtures, which prevented the flame from being displaced by velocity fluctuations.

The channel results exhibit strong deviations from the flashback limits obtained from tube burners with unconfined flames. It is thus necessary to check if the quasi-2D flow situation, the asymmetric flame configuration or some other configuration dependent factors are delusive here. The flashback limits of the confined tube burner can be used as a validation set in this case, since the flow and flame configuration as well as the rig structure are different, the only common ground being the flame stabilization inside the duct section. It can be seen in Fig. 10b that the flashback limits for the confined tube burner strictly follow the channel values for very lean mixtures and also match the offset of the 2 mm step results from channel configuration 3 for increasing Φ. These findings confirm that the increase in flashback propensity observed in the channel is not caused by some peculiarities of the setup, but is a fundamental difference between confined and unconfined flame holding prior to flashback.

Discussion

The large difference between the flashback limits in the established unconfined tube burner setup and the confined setups investigated here is an important finding because it demonstrates that all existing literature results on turbulent flashback limits are non-conservative. The pressure boundary condition normal to the main flow direction is proposed to constitute the physical reason for the deviating flashback behavior. The density jump across the flame causes a static pressure rise upstream of it. Regarding the unconfined burner case, the burner rim quenches the reaction above it. As an effect, the fresh mixture at the inner burner wall is accelerated towards the quenching gap, which leads to the well known overhang of the reaction zone in that region. This situation reduces the flashback propensity for two reasons. On the one hand, the adverse pressure gradient locally imposed on the boundary layer region by the flame anchor is reduced by the pressure drop across the quenching gap. On the other hand, the flame is deterred from entering the boundary layer region due to the outward radial fluid motion.

For a confined flame stabilized at a small backward-facing step, such as the confined tube burner setup used here or configuration 3 of the channel setup, the physical picture is slightly different. The quenching of the chemical reaction causes a gap downstream of the step edge with an associated pressure drop in the same way as for the unconfined case. However, the flow of fresh mixture through this gap is obstructed by the offset channel wall. Thus, with decreasing step height, the fluid motion perpendicular to the main flow direction diminishes and the flame anchor moves closer to the boundary layer region of the fresh mixture. Moreover, the quenching distance is decreasing since a decrease of the gap leakage flow reduces the convective heat loss from the preheat zone of the flame. These two effects result in an increased flashback propensity with decreasing step height, which has been observed experimentally (cf. Fig. 10b).

A confined flame which is stabilized flush with the duct wall, such as in configuration 1 of the channel setup, is always present right inside the boundary layer. Also in this case, streamlines close to the wall are deflected towards the quenching gap below the flame, but this motion does not displace the flame tip appreciably. Furthermore, the quenching distance of this sidewall configuration is known to be smaller than the axial distance between burner rim and an unconfined flame stabilized above it [11]. The results from this configuration can hence be viewed as the upper limit for flashback propensity for a given turbulent boundary layer state.

SUMMARY AND CONCLUSIONS

Turbulent boundary layer flashback limits for fully premixed hydrogen-air flames at atmospheric mixture temperature and pressure have been measured for different geometrical configurations. The velocity gradients at the wall during flashback were documented as a measure for the critical boundary layer state. The results for a tube burner with an unconfined flame burning into the free atmosphere during stable operation compare well to literature results obtained from a similar configuration. As a second set of experiments, the safety-critical situation of a confined flame burning already inside the duct has been investigated. Two experimental rigs were used for this purpose - a tube burner and a rectangular channel with high aspect ratio. The confined tube burner comprised a backward-facing step with a fixed height as flame stabilization. The channel setup comprised either a backward-facing step, where two different step heights were investigated, or a stabilization right inside the boundary layer by means of a hot ceramic tile flush with the channel walls. The flashback limits obtained from the confined experiments are substantially higher than the well-established unconfined results. A good match has been observed between the confined tube burner and the channel results with backward-facing step stabilization. The channel results for flush ceramic tile stabilization lie above all other confined results and mark the upper limit for flashback propensity of flames burning inside the boundary layer of a duct. A physical explanation for the observed differences between confined and unconfined flames has been provided, which proposes the quenching distance between flame and wall, the resulting geometry-dependent leakage flow and the associated flame base shift as well as the reduction of the local pressure gradient in the boundary layer region by the leakage flow to be the determining factors. It is concluded that the distribution of the flame backpressure and the flame position itself are key parameters for the determination of meaningful turbulent boundary layer flashback limits. For a conservative design path, the present results obtained from confined flames with flush flame holding should be considered instead of open tube burner values.

ACKNOWLEDGMENT

Parts of this publication form a part of the BIGCO2 project, performed under the strategic Norwegian research program Climit. The authors acknowledge the partners: StatoilHydro, GE Global Research, Statkraft, Aker Clean Carbon, Shell, TOTAL, ConocoPhillips, ALSTOM, the Research Council of Norway (178004/I30 and 176059/I30) and Gassnova (182070) for their support.

Parts of this publication have been produced with support from the BIGCCS Centre, performed under the Norwegian research program *Centres for Environment-friendly Energy Research (FME)*. The authors acknowledge the following partners for their contributions: Aker Solutions, ConocoPhilips, Det Norske Veritas AS, Gassco AS, Hydro Aluminium AS, Shell Technology AS, Statkraft Development AS, Statoil Petroleum AS, TOTAL E&P Norge AS, and the Research Council of Norway (193816/S60).

REFERENCES

[1] Lewis, B., and von Elbe, G., 1943. "Stability and structure of burner flames". *Journal of Chemical Physics,* ***11***, pp. 75–97.

[2] Caffo, E., and Padovani, C., 1963. "Flashback in premixed air flames". *Combust. & Flame,* ***7***, pp. 331–337.

[3] Fine, B., 1958. "The flashback of laminar and turbulent burner flames at reduced pressure". *Combust. & Flame,* ***2***, pp. 253 – 266.

[4] Fine, B., 1959. "Effect of initial temperature on flash back of laminar and turbulent burner flames". *Ind. Eng. Chem.,* ***51***, pp. 564–566.

[5] Bollinger, L. E., 1952. Studies on burner flames of hydrogen-oxygen mixtures at high pressures. Tech. Rep. WADC Tech. Rep. 52-59, Wright Air Development Center.

[6] Eichler, C., and Sattelmayer, T., 2011. "Experiments on flame flashback in a quasi-2d turbulent wall boundary layer for premixed methane-hydrogen-air mixtures". *Journal of Engineering for Gas Turbines and Power,* ***133***(1), p. 011503.

[7] Khitrin, L., Moin, P., Smirnov, D., and Shevchuk, V., 1965. "Pecularities of laminar- and turbulent-flame flashbacks". In 10th Symposium (International) on Combustion, pp. 1285 – 1291.

[8] Schlichting, H., 1982. *Grenzschicht-Theorie*. Verlag G. Braun.

[9] Kähler, C. J., McKenna, R., and Scholz, U., 2005. “Wall-shear-stress measurements at moderate Re-numbers with single pixel resolution using long distance μ-PIV - an accuracy assessment”. In 6th International Symposium on Particle Image Velocimetry Pasadena, California, USA.
[10] White, F. M., 2005. *Viscous Fluid Flow*. McGraw-Hill.
[11] Wohl, K., 1953. “Quenching, flash-back, blow-off - theory and experiment”. *4th Symp (Int.) on Combustion*, pp. 68 – 89.